

Article

First Report of the Dinoflagellate Genus *Effrenium* in the East Sea of Korea: Morphological, Genetic, and Fatty Acid Characteristics

Nam Seon Kang ¹, Eun Song Kim ¹, Jung A Lee ¹, Kyeong Mi Kim ¹, Min Seok Kwak ¹,
Moongeun Yoon ¹ and Ji Won Hong ^{2,*} 

¹ Department of Taxonomy and Systematics, National Marine Biodiversity Institute of Korea, Seocheon 33662, Korea; kang3610@mabik.re.kr (N.S.K.); kes2523@mabik.re.kr (E.S.K.); jung@mabik.re.kr (J.A.L.); kmkim@mabik.re.kr (K.M.K.); poohaxx@mabik.re.kr (M.S.K.); mgyoon@mabik.re.kr (M.Y.)

² Department of Hydrogen and Renewable Energy, Kyungpook National University, Daegu 41566, Korea

* Correspondence: jwhong@knu.ac.kr; Tel.: +82-(0)53-950-4578; Fax: +82-(0)53-950-3889

Received: 22 March 2020; Accepted: 7 May 2020; Published: 11 May 2020



Abstract: Most species in the family Symbiodiniaceae are symbiotic partners to invertebrate and protist hosts, but a few live freely in water columns. Here, a free-living dinoflagellate was isolated from the waters off the Dokdo Islands in the East Sea of Korea. Morphological and molecular analyses show this isolate belongs to *Effrenium voratum*. Prior to the present study, *E. voratum* had been reported to live in the waters in the temperate latitudes in the western North Pacific, the southwest Western Pacific, the eastern North Pacific, the eastern Atlantic, and the Mediterranean Sea. To our knowledge, this is the highest latitude in the western North Pacific, where *E. voratum* has been reported. This report extends the known range of this dinoflagellate to the temperate waters of the western North Pacific Ocean. The sequence of the D1/D2 region of the large subunit ribosomal DNA (LSU rDNA) was identical to *E. voratum* found in Jeju Island, Korea, Tsushima Island, Japan, and Cook Strait, New Zealand, suggesting this species is cosmopolitan. However, it was different by 1 bp from those found in Blanes, Spain and Santa Barbara, USA. In the phylogenetic tree built on the basis of the LSU (D1-D2) rDNA region sequences, this dinoflagellate was clustered within a clade, including all the other *E. voratum* strains. Morphological characteristics were like those of strains found in the waters of Jeju Island. This is the first report conducted on the fatty acid profile of fully characterized *E. voratum*. Importantly, the isolate possessed a high ratio of long-chain omega-3 polyunsaturated fatty acids (PUFAs) such as eicosapentaenoic acid (EPA) and docosahexaenoic acid (DHA) relative to total lipid. This dinoflagellate could be a candidate for commercial applications, such as aquaculture feed and essential omega-3 PUFA productions.

Keywords: dinoflagellate; Dokdo Islands; *Effrenium voratum*; first record; taxonomy

1. Introduction

Dinoflagellates are ubiquitous protists that can be found in almost every conceivable marine environment [1]. Recently, they have drawn increasing attention from both the scientific and public communities because of the following reasons: Some dinoflagellates form red tides and/or harmful algal blooms, which often cause large-scale mortality of fish [2], they play indispensable ecological roles in marine plankton communities, serving as prey for a variety of predators and as a predator on diverse microorganisms [3], some dinoflagellates are used as various biological resources and they are also treated as one of the most promising bio-resources for new high-value products [4–6]. In particular, dinoflagellates are known to be rich in long-chain omega-3 PUFAs, such as EPA (C_{20:5} n-3) and DHA (C_{22:6} n-3) [7–9]. Thus, the amount and composition of omega-3 PUFAs from dinoflagellates in the phytoplankton community are strongly intertwined with higher trophic levels, eventually affecting

the nutritional values of higher-order consumers [7,10,11]. Therefore, to better understand the role of dinoflagellates in the marine ecosystems and their potential commercial applications, the establishment of a clonal culture is a critical first step for accurate identification of an isolate of interest.

The family Symbiodiniaceae (Order Suessiales) comprises symbiotic dinoflagellates, most of which are symbiotic with invertebrate and protist hosts [12–17], even though some species exist as free-living forms [18]. These dinoflagellates are vital components of the coral reef ecosystems, and they are promising resources in the production of valuable pigments [19] and toxin compounds, such as zooxanthella toxins [20]. Despite their ecological and economic importance in the marine ecosystems and biotechnology, little information is available on their taxonomy. This is due to, in part, the difficulties in culturing and making morphological observations, which must be done by scanning electron and transmission electron microscopy (SEM and TEM). Therefore, their roles as essential components of the marine ecosystems and their potential for biotechnology are often overlooked. Accurate identification and establishment of a clonal culture of these dinoflagellates are essential for further research and commercial application.

The systematics of Symbiodiniaceae was revised, and distinct clades within the family were reassigned into seven genera in 2018 [21]. *Symbiodinium voratum* was first described and named by Jeong et al. [18], it was renamed as *Effrenium voratum* by LaJeunesse et al. [21]. This is the only taxonomically accepted species in the genus *Effrenium* [21]. *E. voratum* is found in the Pacific and Atlantic Oceans, and it grows at sub-tropical and temperate latitudes [18,21–24]. Jeong et al. [18] reported the Korean *E. voratum* strains that had been isolated from waters off Jeju Island. However, no additional documentation of *E. voratum* colonies in Korean water have been reported.

In this study, we isolated and identified a unicellular dinoflagellate *E. voratum* from seawater off the Dokdo Islands, Dokdo-ri, Ulleung-eup, Ulleung-gun, Gyeongsangbuk-do, Korea. The present report provides information about the morphological, molecular, and chemotaxonomic features on the first record of this species living in the East Sea of Korea.

2. Materials and Methods

2.1. Sample Collection and Isolation

Plankton samples from the Dokdo Islands in the East Sea of Korea (37.240486 N, 131.870853 E), were collected using a water sampler during September 2016, when the water conditions were 24 °C and 35 practical salinity unit (PSU), respectively (Table 1, Figure 1). The samples were gently filtered through a 154 µm Nitex mesh and placed in six-well tissue culture plates. A clonal culture of *E. voratum* was established by using two serial single-cell isolations. Polycarbonate (PC) bottles containing f/2 medium (AusAqua, Wallaroo, SA, Australia) and isolated *E. voratum* cells were filled with filtered seawater, capped, and incubated at 20 °C, under illumination by cool white fluorescent lights at approximately 20 µmol photons m⁻² s⁻¹ in a 14:10 h light-dark cycle. As the concentration of *E. voratum* increased, the cells were transferred to 50, 125, and 500 mL PC bottles containing fresh f/2 media. Once dense cultures of *E. voratum* were obtained, they were transferred approximately every four weeks to new 500 mL PC bottles filled with fresh f/2 media. When sufficient volumes of *E. voratum* culture were available, genomic DNA was extracted, and the DNA sequence of the cultured cells was analyzed. After genetic identification, the morphology and cellular fatty acid composition of the dinoflagellate were examined. For morphological and fatty acid analyses, cells were collected in the exponential growth phase.

Table 1. Strain, location of the collection (LC), water temperature (T, °C), salinity (S, PSU), and GenBank accession number (GBAN) for rDNA sequences of *E. voratum* MABIKLP88 isolated from the Dokdo Islands, in the East Sea of Korea.

Species	Strain	LC	Date	T	S	GBAN
<i>E. voratum</i>	MABIKLP88	Dokdo Islands	September 2016	24	35	MN904916

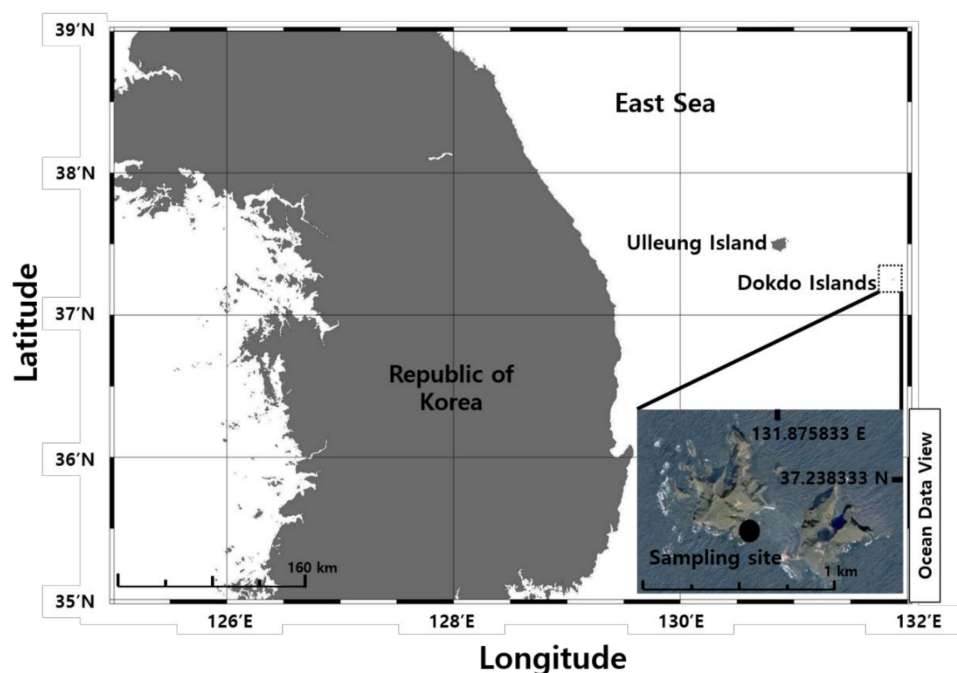


Figure 1. Location of the sampling site in the coastal area of the Dokdo Islands, Korea. The large map template was taken from the Ocean Data View, and the small map was generated from Google Earth.

2.2. Morphological Identification

An inverted microscope was used to examine the morphology of photosynthetically grown living cells. The length and width of the live cells were measured with the aid of a digital camera (Zeiss AxioCam MRC5; Carl Zeiss, Göttingen, Germany). For SEM, 10 mL aliquots of cultures at ~ 1000 cells mL^{-1} were fixed for 10 min in osmium tetroxide (OsO_4 ; Electron Microscopy Sciences, EMS hereafter, Hatfield, PA, USA) at a final concentration of 2% (v/v) in seawater. Fixed cells were collected on a 3 μm pore-sized PC membrane filter without additional pressure and rinsed three times with distilled water to remove residual salts. Cells were dehydrated in an ethanol series (Merck, Darmstadt, Germany) and dried using a critical point dryer (CPD 300, Bal-Tec, Balzers, Liechtenstein). The dried filters were mounted on a stub and coated with gold-palladium in a sputter coater (SCD 005; Bal-Tec). Cells were viewed with an FE-SEM (S-4800; Hitachi, Hitachinaka, Japan). For TEM, cells from a dense culture were transferred to a 10 mL tube and fixed in 2.5% (v/v) glutaraldehyde (final concentration, EMS) in a culture medium. After 1.5–2 h, the contents of the tube were placed in a 10 mL centrifuge tube and concentrated at $1610\times g$ for 10 min in a Vision Centrifuge VS-5500 (Vision Scientific, Bucheon, Korea). The pellet was transferred to a 1.5 mL tube and rinsed in 0.2 M sodium cacodylate buffer (EMS) at pH 7.4. After several rinses in the buffer, cells were post-fixed for 1.5 h in 1% (w/v) OsO_4 in deionized water. The pellet was embedded in agar (EMS) and dehydrated in a graded ethanol series (50%, 60%, 70%, 80%, 90%, and 100% ethanol, followed by two changes in 100% ethanol). The material was embedded in Spurr's low-viscosity resin (Low Viscosity Embedding Media Spurr's Kit; EMS). Sections were prepared on an RMC MT-XL ultramicrotome (Boeckeler Instruments, Tucson, AZ, USA) and stained using 3% (w/v) aqueous uranyl acetate (EMS) followed by lead citrate (EMS). The sections were viewed using a JEOL-1010 TEM (Tokyo, Japan).

2.3. Molecular Identification

For molecular analysis, approximately 10 mL of a dense *E. voratum* culture was concentrated by centrifugation at $2190\times g$ for 15 min at room temperature, and the pellet was used for genomic DNA extraction. The DNA extraction, including the amplification of the LSU rDNA, PCR reaction, sequencing, and alignment of DNA sequences, were performed as previously reported by Kang et al. [25]. The primers that were used to amplify the LSU region of rDNA are reported in Table 2.

Table 2. Oligonucleotide primers and sequences used in this study to amplify the LSU region of rDNA of *E. voratum*.

Primer Name	Amplifies	Sequence (5'-3')	Reference
Forward primer D1R	LSU rDNA	ACC CGC TGA ATT TAA GCA TA	[26]
Reverse primer LSUB	LSU rDNA	ACG AAC GAT TTG CAC GTC AG	[27]

Alignments, phylogenetic, and molecular evolutionary analyses of the D1-D2 LSU rDNA sequences were performed using MEGA v.4 [28] and Clustal X2 [29], with diverse assemblages using available data in the National Center for Biotechnology Information (NCBI) GenBank database, for other species. Bayesian analyses were performed using MrBayes v.3.1 [30,31] with the default GTR + G + I model, to determine the best model for the data in each region. For all sequence regions, four independent Markov Chain Monte Carlo (MCMC) runs were performed, as described by Kang et al. [32]. Maximum likelihood (ML) analyses were conducted using the RAxML 7.0.3 program [33]. We allowed for 200 independent free inferences and used the *-#* option to identify the best tree. Bootstrap values were calculated using 1000 replicates under the same substitution model.

2.4. Fatty acid Composition Analysis

Lipid extraction was carried out using the modified Bligh-Dyer method developed by Breuer et al. [34]. Fatty acid methyl ester (FAME) composition was analyzed using a 7890A gas chromatograph, equipped with a 5975C mass selective detector (Agilent, Santa Clara, CA, USA), based on our previous publication [35]. Compound identification was completed by matching the mass spectra with those in the Wiley/NBS registry of mass spectral data, searches with a match value higher than 90% were valid.

3. Results

Mastigote, coccoid, and doublet cells occurred in all cultures examined under light microscopy, and they appeared to be like one another (Figure 2A–C). Motile cells of *E. voratum* were mushroomed-shaped with the hemispherical episome slightly larger than the hemispherical hyposome (Figure 2A). The nucleus was in the episome (Figure 2A). The ranges (mean \pm standard error, $n = 30$) of the living cell length and width were 9.42–15.6 μm (12 ± 0.2) and 7.08–11.9 μm (9.7 ± 0.2), respectively (Table 3). The ratios of the cell length to the width (mean \pm standard error, $n = 30$) ranged from 1.12 to 1.4 (1.2 ± 0.01). When observed under SEM, fixed cells were slightly smaller than unfixed cells. The cell length under SEM had a range of 7.3–12.7 μm (9.6 ± 0.2) and the width had a range of 5.52–11.4 μm (7.7 ± 0.2), respectively (Table 3). The ratio of the length to the width under SEM had a range of 0.83–1.4 μm (1.2 ± 0.02) (Table 3).

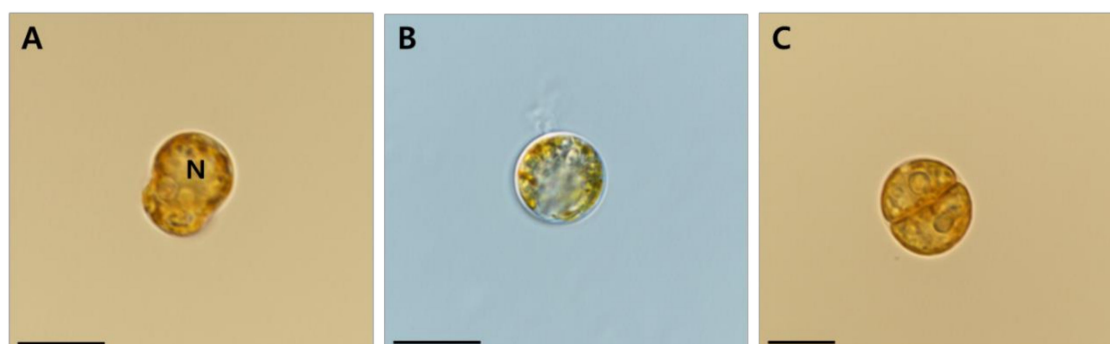


Figure 2. Light micrographs of the mastigote (motile), coccoid (spherical), and doublet (dividing) cells from *E. voratum*. (A) *E. voratum* mastigote, nucleus (N). (B) *E. voratum* coccoid. (C) *E. voratum* doublet. Scale bars: A–C = 10 μm .

Table 3. Morphological comparisons of mastigotes from strains MABIKLP88, SvFL 1, and CCMP421.

Mastigote Character Traits	MABIKLP88	SvFL 1	CCMP421
Strain locality	Dokdo Islands, Korea	Jeju Island, Korea	Cook Strait, New Zealand
Shape in ventral view	Mushroom	Mushroom	Mushroom
AP length (μm ; living cells)	9.42–15.6 (12)	10.8–16.2 (13.1)	10.1–17.1 (12.8)
Cell width (μm ; living cells)	7.08–11.9 (9.7)	7.8–11.5 (9.5)	8.1–14.4 (10.3)
Ratio of length to width (living cells)	1.12–1.4 (1.2)	1.1–1.8 (1.4)	1.2–1.3 (1.2)
AP length (μm ; SEM)	7.3–12.7 (9.6)	8.5–12.4 (10.5)	7.0–13.0 (11.7)
Cell width (μm ; SEM)	5.52–11.4 (7.7)	6.4–9.8 (8.2)	5.8–10.9 (9.2)
Ratio of length to width (SEM)	0.83–1.4 (1.2)	1.2–1.4 (1.3)	1.2–1.4 (1.3)
EAV length (μm)	1.71–2.72 (2.25)	1.75–3.09 (2.45)	1.98–3.19 (2.64)
EAV width (μm)	0.15–0.26 (0.21)	0.15–0.27 (0.2)	0.18–0.29 (0.22)
Numbers of aligned knobs on EAV	11–12	9–13	9–13
Cingulum displaced by cell length	0.11–0.26 (0.18)	0.13–0.21 (0.15)	0.10–0.19 (0.15)
Cingulum displaced by cell width	0.49–0.80 (0.62)	0.48–0.85 (0.65)	0.55–1.10 (0.78)
Numbers of cingular plates	17–20	17–20	17–20
Numbers of sulcal plates	9	9	9
Numbers of apical plates	5	5	5
Numbers of intercalary plates	5	5	5
Numbers of precingular plates	8	8	8
Numbers of postcingular plates	6	6	6
Numbers of antapical plates	2	2	2
Existence of eyespot type E	Yes	Yes	Yes
Plate formula	x, EAV, 5', 5a, 8'', 9s, 17–20c, 6''', 2''''', PE	x, EAV, 5', 5a, 8'', 9s, 17–20c, 6''', 2''''', PE	x, EAV, 5', 5a, 8'', 9s, 17–20c, 6''', 2''''', PE
Reference	This study	[18]	[18]

Mean values are shown in parentheses. AP = anteroposterior; EAV = elongated amphiesmal vesicle, PE = peduncle.

Mastigote, coccoid, and doublet cells were present in all cultures under SEM observation (Figures 3 and 4). Mastigotes possessed a well-formed peduncle (PE) extending near the base of the longitudinal (LF) and transverse flagella (TF) (Figure 3B). The Kofoidian plate formula of *E. voratum* cells was x, elongated amphiesmal vesicle (EAV), 5', 5a, 8'', 9s, two cingulum rows 17–20c, 6''', and 2'''' (Table 3, Figure 4). At the cell's apex, the EAV possessed 11–12 aligned knobs, and the length had a range of 1.71–2.72 μm (2.25 ± 0.11) and the width had a range of 0.15–0.26 μm (0.21 ± 0.01) (Table 3). This structure was bordered ventrally, by the x plate and surrounded by four apical amphiesmal plates (2', 3', 4', and 5' plates; Figure 4E,F). The rhomboid-shaped 1' plate was relatively large and the quadrangular 2' plate was relatively small (Figure 4E). The pentagonal 3' plate touched the 2', 4', 1a, and 2a plates and the pentagonal 4' plate touched the 3', 5', 2a, 3a, and 4a (Figure 4C,E,F). The pentagonal 5' plate touched the x, 4', 4a, and 5a plates (Figure 4C,E,F). Eight pre-cingular plates were present (Figure 4A–E). The 1'', 4'', and 6'' plates were quadrangular, while the 2'', 3'', 5'', 7'', and 8'' were pentagonal. In addition, five intercalary plates were observed (Figure 4A–F). Cells of *E. voratum* had a wide cingulum comprising of two rows of pentagonal amphiesmal plates (Figure 4A–D). Cells contained 17–20 cingular plates (Table 3). The cingulum of *E. voratum* was displaced by ~0.1–0.3 times the cell length and by ~0.5–0.8 times the cingular width (Table 3, Figure 4A). The cells of *E. voratum* contained six post-cingular plates (Figure 4G). Except for the pentagonal 3''' plate, all post-cingular plates were quadrangular (Figure 4G). Two antapical plates were present in the cells of *E. voratum* (Figure 4G). The 2'''' plates in most cells were hexagonal, and they touched the 3''', 4''', 5''', 6''', and 1'''' plates and the posterior sulcal plate (S.p.) (Figure 4A,G).

single-base substitution in LSU compared to strain MABIKLP88 (Table 4). In the phylogenetic tree based on the LSU rDNA sequences, the phylogenetic diversity was presently divided into seven distinct monophyletic groups (clades A-G). The *Effrenium* clade E was phylogenetically basal of clade B, C, D, F, and G (Figure 6). In addition, *E. voratum* strain MABIKLP88 formed a big clade (i.e., *Effrenium* clade E) with strains SVIC1, SVFL1-6, TSP-C2-Sy, CCMP 421, RCC 1521, and rt-383 (Figure 6).

The major FAME profile of the isolate was C_{16:0} (22.1%), C_{18:4} n-3 (15.2%), C_{20:5} n-3 (10.9%), and C_{22:6} n-3 (25.4%) (Table 5). Trace amounts of saturated fatty acids (SFAs, C_{12:0}, 0.6%; C_{14:0}, 3.5%; C_{15:0}, 0.3%; C_{18:0}, 0.7%), unsaturated fatty acids (C_{16:1} n-7, 9.3%; C_{16:2} n-4, 0.4%; C_{18:1} n-9, 3.3%; C_{18:2} n-6, 0.6%; C_{18:3} n-6, 0.9%; C_{18:3} n-3, 0.3%), and unidentified fatty acids (6.5%), were detected (Table 5).

Table 4. Comparison of LSU rDNA sequence of *E. voratum* MABIKLP88 isolated from the Dokdo Islands, in the East Sea of Korea and other strains. The numbers indicate the number of base pairs that differ between strains. The numbers in parentheses indicate dissimilarity (%), including gaps.

Collection Location	Strain	GenBank Accession No.	<i>E. voratum</i> MABIKLP88
Jeju Island, Korea	SVIC1	HE653239	0 (0)
	SVFL1	HF568830	0 (0)
	SVFL2	HF568831	0 (0)
	SVFL3	HF568832	0 (0)
	SVFL4	HF568833	0 (0)
	SVFL5	HF568834	0 (0)
Tsushima Island, Japan	SVFL6	HF568835	0 (0)
Cook Strait, New Zealand	TSP-C2-Sy	KF364604	0 (0)
Blanes, Spain	CCMP421	KF364603	0 (0)
Santa Barbara, CA, USA	RCC1521	KF364606	1 (0.2)
	rt-383	KF364605	1 (0.2)

Table 5. Lipid profile of strain MABIKLP88.

Component	Content (%)	Note
Lauric acid (C _{12:0})	0.6	
Myristic acid (C _{14:0})	3.5	
Pentadecanoic acid (C _{15:0})	0.3	
Palmitic acid (C _{16:0})	22.1	SFA (major)
Palmitoleic acid (C _{16:1} n-7)	9.3	
Hexadecadienoic acid (C _{16:2} n-4)	0.4	
Stearic acid (C _{18:0})	0.7	
Oleic acid (C _{18:1} n-9)	3.3	
Linoleic acid (C _{18:2} n-6)	0.6	
g-linolenic acid (C _{18:3} n-6)	0.9	
α-linolenic acid (C _{18:3} n-3)	0.3	
Stearidonic acid (C _{18:4} n-3)	15.2	Omega-3 PFUA (major)
Eicosapentaenoic acid (C _{20:5} n-3)	10.9	Omega-3 PFUA (major)
Docosahexaenoic acid (C _{22:6} n-3)	25.4	Omega-3 PFUA (major)
Unidentified	6.5	

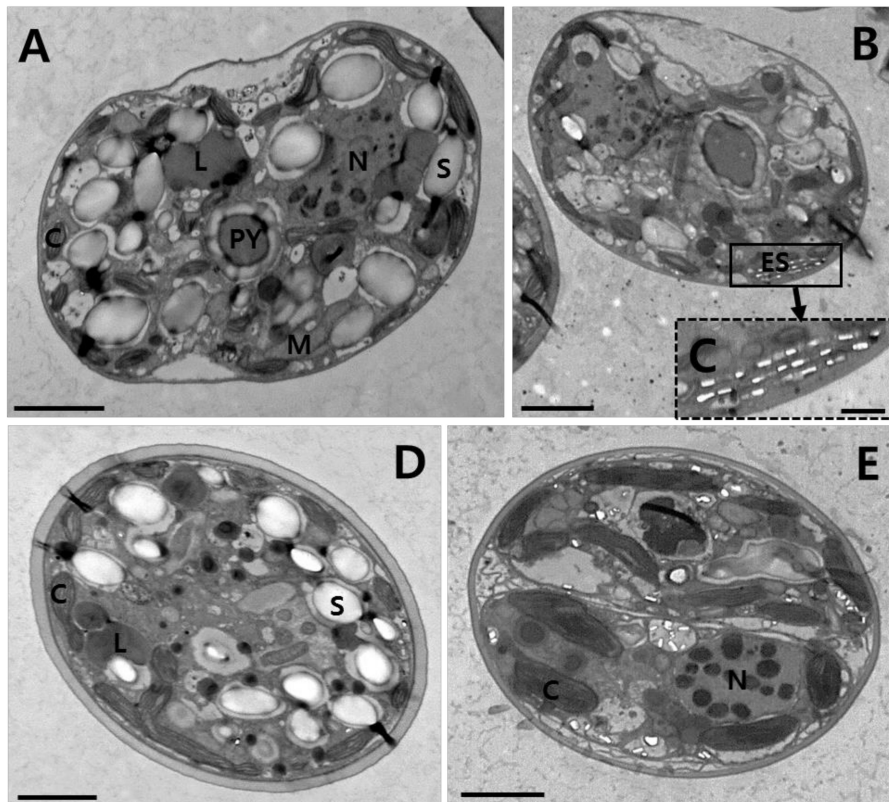


Figure 5. Transmission electron micrographs of *E. voratum* cells. (A) A transverse section of a mastigote cell from *E. voratum* showing the position of the pyrenoid (PY) in the middle of the cell, the chloroplasts (C), lipid globules (L), mitochondria (M), nucleus (N), and starch (S). (B) A magnified view of the type E eyespot (ES) composed of multiple layers of rectangular electron-translucent vesicles, or crystalline deposits. (C) TEM figure enlarged from Figure B, showing the type E eyespot. (D) *E. voratum* coccioid. Micrograph showing a chloroplast (C), lipid globules (L), and starch (S). (E) *E. voratum* doublet. Micrograph showing a chloroplast (C) and nucleus (N). Scale bars: A, B, D, E = 2 μm , C = 0.5 μm .

4. Discussion

The key for differentiating families in the order Suessiales [36] is the morphology of the apical furrow: Species in the family Tovelliaceae have an apical line of narrow plates (ALP), species in the family Borghiellaceae have a pair of elongated anterior vesicles (PEV), and species in the family Symbiodinaceae have a single EAV [37]. All Symbiodinaceae contain a type E eyespot next to the sulcus groove of the motile cell. The motile stage (mastigote) has only seven latitudinal series of amphiesmal vesicles [21]. Strain MABIKLP88 had the EAV, type E eyespot, and seven latitudinal series of amphiesmal vesicles, these morphologies fit the criteria for the family Symbiodinaceae.

The morphological features of this isolate resembled those of the strain SvFL 1 and CCMP421 because it had a type E eyespot, a peduncle, two-stalked pyrenoid, peripheral chloroplasts, and a Kofoidian series of the small plate (x), the EAV, 5', 5a, 8'', 9s, 17-20c, 6''', and 2'''' (Table 3). The length and the width of living *E. voratum* MABIKLP88 cells were 9.42–15.6 μm and 7.08–11.9 μm , respectively. The sequence of the D1/D2 region of LSU rDNA was also identical to those of strains SvFL 1 and CCMP421 (Table 4). Although these *E. voratum* strains were isolated from distinct sites (the Dokdo Islands in Korea, Jeju Island in Korea, and Cook Strait in New Zealand), they all share the typical morphologies of *E. voratum* and identical LSU rDNA sequences. Thus, this newly isolated Korean strain could serve as a good example of a cosmopolite species found in different oceans. The length and width of living cells of the *E. voratum* MABIKLP88 (9.42–15.6 μm and 7.08–11.9 μm , respectively) were comparable to those of other strains of *E. voratum* reported at 10.1–17.1 μm and 7.8–14.4 μm , respectively (Table 3). In SEM micrographs of cells, the width and EAV length of the *E. voratum* MABIKLP88 (5.52–11.4 μm and 1.71–2.72 μm , respectively) were also similar to those of other strains of *E. voratum* (5.8–10.9 μm and 1.75–3.19 μm , respectively) (Table 3). The ratio of cell length to the width of the *E. voratum* MABIKLP88 (0.83–1.4) was comparable to those of other strains of *E. voratum* (1.2–1.4) (Table 3). The ratio of cingulum displacement to cell length of the *E. voratum* MABIKLP88 (0.11–0.26) was similar to those of other strains of *E. voratum* (0.1–0.21) (Table 3). Therefore, our report provides new information on the extended ranges of cell length, cell width, EAV length, the ratio of cell length to cell width, and the ratio of cingulum displacement to cell length in *E. voratum*. These results showed more variability on the measured morphological traits of the species than previously reported *E. voratum* strains.

The sequence of the D1/D2 region of LSU rDNA was identical to the of the *E. voratum* strains located in the waters off the Jeju Island of Korea, Tsushima Island of Japan, and Cook Strait of New Zealand. Our phylogenetic analysis confirmed that the strain MABIKLP88 belonged to *E. voratum* (Table 4, Figure 6). Molecular phylogeny results from the LSU rDNA sequences supported the morphological identification by forming a well-supported clade, including the sequences from the original description.

Prior to the present study, *E. voratum* had been reported to live in waters in the temperate latitudes in the western North Pacific, the southwest Western Pacific, the eastern North Pacific, the eastern Atlantic, and the Mediterranean Sea [18,21–24,38–40]. *E. voratum* appears to be distributed across high sub-tropical and low temperate latitudes. *E. voratum* is cold-water-adapted and may tolerate temperatures as low as 10–12 $^{\circ}\text{C}$. This is supported by physiological measurements taken on culture rt-383, which showed that this strain grew optimally at 15–20 $^{\circ}\text{C}$, but also grew at 12 $^{\circ}\text{C}$ and 28 $^{\circ}\text{C}$ [41]. This wide temperature range tolerance may enable *E. voratum* to survive in a wide variety of oceanic environments around the world (Figure 7). Additional physiological tests on rt-383 and other *E. voratum* strains are needed to elucidate their thermal tolerance. In addition, the maximal growth of strain MABIKLP88 was obtained at 22–28 $^{\circ}\text{C}$ and 300–700 $\mu\text{mol photons m}^{-2} \text{s}^{-1}$ (unpublished data). Moreover, *E. voratum* has an ability to feed on bacteria and other macroalgae, proving a possible survival strategy for *Effrenium* to persist in nutrient-poor conditions [39].

It seems that this wide temperature range tolerance of the species, coupled with tolerance to high light intensities and mixotrophic ability, attributed to *E. voratum*'s survival and presence in a wide variety of oceanic environments around the world. Thus, this newly isolated Korean strain could

serve as a good example of a candidate for cosmopolite species in high sub-tropical and low temperate latitudes. Exploration of this dinoflagellate's distribution in greater detail would be worthwhile.

As shown in Figure 7, *E. voratum* strains are present in many locations, and the current report further describes the occurrence of *E. voratum* in the western North Pacific Ocean (Table 6, Figure 7). The latitude of the Dokdo Islands, where strain MABIKLP88 was isolated, is 37.2 N. The locations where additional stains of the western North Pacific have been reported range from 22.5 N to 36.0 N (Table 6). To date, the waters around the Dokdo Islands are the highest latitude in the western North Pacific, where *E. voratum* has been found. The findings in this report expand upon the understanding of the geographic distribution of *E. voratum* in the western North Pacific. It may also show that climate changes caused by global warming have taken place in the oceans around the Korean Peninsula since the Dokdo Islands are located at the front between the warm Kuroshio and the cold Kuril currents.

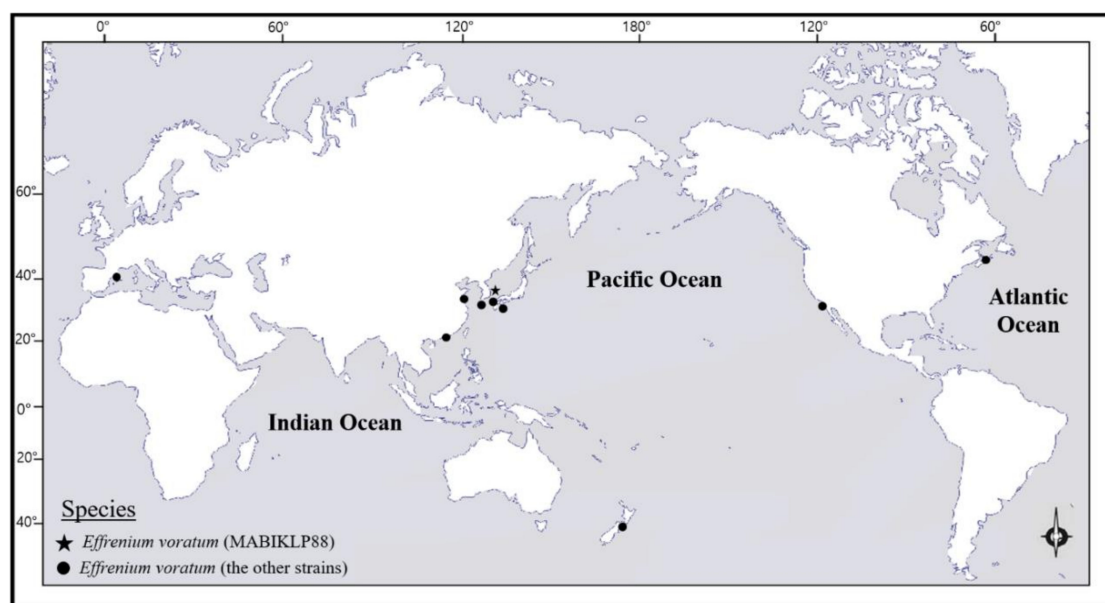


Figure 7. The global distribution of *E. voratum*. The dark circles refer to previous [18,21–24,38–40], while the dark star indicates our MABIKLP88 strain of *E. voratum*.

Table 6. Strains of *E. voratum* isolated from locations in the western North Pacific Ocean.

Culture	Collection Region	LC	Latitude	Longitude	Reference
MABIKLP88	Western North Pacific	Dokdo Islands, South Korea	37.240486 N	131.870853 E	This study
SvIC 1	Western North Pacific	Jeju Island, South Korea	33.276667 N	126.170556 E	[39]
SvFL 1	Western North Pacific	Jeju Island, South Korea	33.468611 N	126.324444 E	[39]
SvFL 2–5	Western North Pacific	Jeju Island, South Korea	33.277778 N	126.719067 E	[39]
SvFL 6	Western North Pacific	Jeju Island, South Korea	33.276667 N	126.170556 E	[18]
MJa-B6-Sy	Western North Pacific	Muroto Cape, Kochi, Japan Tsushima	33.25 N	134.166667 W	[24]
TSP-C2-Sy	Western North Pacific	Island, Nagasaki, Japan	34.183333 N	129.283333 E	[24]
-	Western North Pacific	Jiaozhou Bay, China	36.02575 N	120.290231 E	[38]
-	Western North Pacific	Zhujiang River estuary, China	22.483333 N	113.75 E	[40]

Analysis of the cellular fatty acid composition of the strain MABIKLP88 revealed that it was rich in C_{16:0} (22.1%), SFA and C_{18:4} n-3 (15.2%), C_{20:5} n-3 (10.9%), and C_{22:6} n-3 (25.4%) PUFAs. The fatty acid profile of different dinoflagellate species has been extensively studied in order to find valuable strains with high potentials for commercial applications [7,8,42–46]. The profile has also been used as a general chemotaxonomic guide to defining a variety of taxonomic groups since different microalgal groups show distinct fatty acid distributions [44,47,48]. In particular, the C₁₈ fatty acids and >C₂₀ PUFAs are generally regarded as the signature fatty acids for dinoflagellates [8,48]. In this study, *E. voratum* MABIKLP88 was found to be rich in the C₁₈ fatty acid, EPA, and DHA. It has also been reported that dinoflagellates typically have higher DHA than EPA concentrations [7–9], and the isolate exhibited much higher DHA (25.4%) content than EPA (10.9%). Several previous studies have shown that the essential omega-3 PUFAs have a variety of beneficial health effects [49]. Importantly, EPA and DHA, which are known essential omega-3 fatty acids, have been reported to be beneficial to human health [50,51]. Most of the omega-3 PUFAs come from marine sources, such as fish oils and a variety of commercial products that are available worldwide. Using marine fish as a sustainable and safe resource of omega-3 is in question because of global climate change, overfishing issues, and the increasing levels of environmental pollutants, such as heavy metals and radioactive materials found in the ocean [52,53]. Some marine protists have high contents of EPA and/or DHA [6,54–57]. Therefore, this marine microalga may have the potential to be a clean and sustainable omega-3 source alternative to fish-based oil. On the other hand, an excessive intake of omega-6 causes negative health outcomes [58,59], even though both omega-3 and omega-6 PUFAs are essential, and they are required for many biological processes. Due to the ever-growing demands for food, the fish farming industry has rapidly expanded over the last few decades and aquaculture now accounts for over 50% of the fish consumed worldwide [60]. This has caused further shortage of wild fish as feed at fish farms, and thus, fish oil in the aquaculture feed has been increasingly replaced by terrestrial vegetable oils that normally lack EPA and DHA, but often contain high levels of omega-6 PUFAs [61]. The imbalance between omega-3 and omega-6 levels has deteriorated the nutritional quality of farmed fish such as Atlantic salmon that contains less EPA and DHA and more omega-6 PUFAs than before [62,63]. Thus, strain MABIKLP88 could be used for the production of designed aquafeeds for balancing the dietary omega-6 and omega-3 ratios. Furthermore, several authors reported that the amount of omega-3 PUFAs in the phytoplankton community is reflected in the nutritional quality of predatory fish [7,10,11]. It should also be noted that the availability of omega-3 PUFAs in aquatic ecosystems is closely related to egg production and hatching success of marine copepods [64,65] and the fish larvae survival [66]. Hence, the presence and abundance of this Korean dinoflagellate may have a potentially positive impact on the sustainability of both capture fisheries and aquaculture in Korea.

In this study, we report the first record of *E. voratum* from the Dokdo Islands, in the East Sea of Korea. This marine dinoflagellate would serve as potential biological resources to produce aquaculture feeds and biochemicals of commercial interests. Importantly, a clonal culture was established and deposited in a national culture collection to allow for further research.

Author Contributions: Conceptualization, N.S.K. and J.W.H.; methodology, N.S.K., J.A.L. and E.S.K.; software, N.S.K. and M.S.K.; validation, K.M.K., M.S.K. and M.Y.; investigation, J.A.L. and E.S.K.; resources, E.S.K.; data curation, N.S.K. and K.M.K.; writing—original draft preparation, N.S.K.; writing—review & editing, J.W.H.; visualization, N.S.K.; supervision, J.W.H.; project administration, K.M.K.; funding acquisition, M.Y. All authors have read and agreed to the published version of the manuscript.

Funding: This work was supported by the Efficient Securement of Marine Bioresources and Taxonomic Research (2020M00100) funded by the National Marine Biodiversity Institute of Korea (MABIK). This research was also supported by a grant from the Marine Biotechnology Program (20170488) funded by the Ministry of Oceans and Fisheries, Korea.

Conflicts of Interest: The authors declare no conflict of interest.

References

1. Jeong, H.J. The Interactions between Microzooplanktonic Grazers and Dinoflagellates Causing Red Tides in the Open Coastal Waters off Southern California. Ph.D. Thesis, University of California, San Diego, CA, USA, 1995; p. 139.
2. Park, T.G.; Lim, W.A.; Park, Y.T.; Lee, C.K.; Jeong, H.J. Economic impact, management and mitigation of red tides in Korea. *Harmful Algae* **2013**, *30*, S131–S143. [[CrossRef](#)]
3. Jeong, H.J.; Yoo, Y.D.; Kim, J.S.; Seong, K.A.; Kang, N.S.; Kim, T.H. Growth, feeding and ecological roles of the mixotrophic and heterotrophic dinoflagellates in marine planktonic food webs. *Ocean Sci. J.* **2010**, *45*, 65–91. [[CrossRef](#)]
4. Hwang, B.S.; Yoon, E.Y.; Kim, H.S.; Yih, W.; Park, J.Y.; Jeong, H.J.; Rho, J. Ostreol A: A new cytotoxic compound isolated from the epiphytic dinoflagellate *Ostreopsis* cf. *ovata* from the coastal waters of Jeju Island, Korea. *Bioorg. Med. Chem. Lett.* **2013**, *23*, 3023–3027. [[PubMed](#)]
5. Jang, S.H.; Jeong, H.J.; Kwon, J.E. High contents of eicosapentaenoic acid and docosahexaenoic acid in the mixotrophic dinoflagellate *Paragymnodinium shiwhaense* and identification of putative omega-3 biosynthetic genes. *Algal Res.* **2017**, *25*, 525–537. [[CrossRef](#)]
6. Yoon, E.Y.; Park, J.Y.; Jeong, H.J.; Rho, J. Fatty acid composition and docosahexaenoic acid (DHA) content of the heterotrophic dinoflagellate *Oxyrrhis marina* fed on dried yeast: Compared with algal prey. *Algae* **2017**, *32*, 67–74. [[CrossRef](#)]
7. Peltomaa, E.; Hällfors, H.; Taipale, S.J. Comparison of diatoms and dinoflagellates from different habitats as sources of PUFAs. *Mar. Drugs* **2019**, *17*, 233. [[CrossRef](#)]
8. Jónasdóttir, S.H. Fatty acid profiles and production in marine phytoplankton. *Mar. Drugs* **2019**, *17*, 151. [[CrossRef](#)]
9. Galloway, A.W.; Winder, M. Partitioning the relative importance of phylogeny and environmental conditions on phytoplankton fatty acids. *PLoS ONE* **2015**, *10*, e0130053. [[CrossRef](#)]
10. Taipale, S.J.; Vuorio, K.; Strandberg, U.; Kahilainen, K.K.; Järvinen, M.; Hiltunen, M.; Peltomaa, E.; Kankaala, P. Lake eutrophication and brownification downgrade availability and transfer of essential fatty acids for human consumption. *Environ. Int.* **2016**, *96*, 156–166. [[CrossRef](#)]
11. Brett, M.T.; Müller-Navarra, D.C.; Ballantyne, A.P.; Ravet, J.L.; Goldman, C.R. *Daphnia* fatty acid composition reflects that of their diet. *Limnol. Oceanogr.* **2006**, *51*, 2428–2437. [[CrossRef](#)]
12. LaJeunesse, T.C. Diversity and community structure of symbiotic dinoflagellates from Caribbean coral reefs. *Mar. Biol.* **2002**, *141*, 387–400.
13. Lee, S.Y.; Jeong, H.J.; Kang, N.S.; Jang, T.Y.; Jang, S.H.; LaJeunesse, T.C. *Symbiodinium tridacnidorum* sp. nov., a dinoflagellate common to Indo-Pacific giant clams, and a revised morphological description of *Symbiodinium microadriaticum* Freudenthal, emended Trench & Blank. *Eur. J. Phycol.* **2015**, *50*, 155–172.
14. Lee, S.Y.; Jeong, H.J.; Kang, N.S.; Jang, T.Y.; Jang, S.H.; Lim, A.S. Morphological characterization of *Symbiodinium minutum* and *S. psymophilum* belonging to clade B. *Algae* **2014**, *29*, 299–310.
15. Lobban, C.S.; Schefter, M.; Simpson, A.G.B.; Pochon, X.; Pawlowski, J.; Foissner, W. *Maristentor dinoferus* n. gen., n. sp. a giant heterotrich ciliate (Spirotrichea: Heterotrichida) with zooxanthellae, from coral reefs on Guam, Mariana Islands. *Mar. Biol.* **2002**, *40*, 411–423.
16. Pochon, X.; Garcia-Cuevas, L.; Baker, A.C.; Castella, E.; Pawlowski, J. One-year survey of a single Micronesian reef reveals extraordinarily rich diversity of *Symbiodinium* types in soritid foraminifera. *Coral Reefs* **2007**, *26*, 867–882. [[CrossRef](#)]
17. Trench, R.K. Microalgal-invertebrate symbioses: A review. *Endocytobiosis Cell Res.* **1993**, *9*, 135–175.
18. Jeong, H.J.; Lee, S.Y.; Kang, N.S.; Yoo, Y.D.; Lim, A.S.; Lee, M.J.; Kim, H.S.; Yih, W.; Yamashita, H.; LaJeunesse, T.C. Genetics and morphology characterize the dinoflagellate *Symbiodinium voratum*, n. sp., (Dinophyceae) as the sole representative of *Symbiodinium* clade E. *J. Eukaryot. Microbiol.* **2014**, *61*, 75–94. [[CrossRef](#)]
19. Lee, S.B. Isolation and Structure Determination of Bioactive Secondary Metabolites from Benthic Marine Dinoflagellates and Sponges. Master's Thesis, Kunsan National University, Gunsan, Korea, 2016.
20. Nakamura, H.; Asari, T.; Ohizumi, Y.; Kobayashi, J.; Yamasu, T.; Murai, A. Isolation of zooxanthellatoxins, novel vasoconstrictive substances from the zooxanthella *Symbiodinium* sp. *Toxicon* **1993**, *31*, 371–376. [[CrossRef](#)]

21. LaJeunesse, T.C.; Parkinson, E.J.; Gabrielson, P.W.; Jeong, H.J.; Reimer, J.D.; Voolstra, C.R.; Santos, S.R. Systematic revision of Symbiodiniaceae highlights the antiquity and diversity of coral endosymbionts. *Curr. Biol.* **2018**, *28*, 2570–2580. [[CrossRef](#)]
22. Chang, F.H. Winter phytoplankton and microzooplankton populations off the coast of Westland, New Zealand, 1979. *N. Z. J. Mar. Freshw. Res.* **1983**, *17*, 279–304. [[CrossRef](#)]
23. Polne-Fuller, M. A novel technique for preparation of axenic cultures of *Symbiodinium* (Pyrrophyta) through selective digestion by amoebae. *J. Phycol.* **1991**, *27*, 552–554. [[CrossRef](#)]
24. Yamashita, H.; Koike, K. The genetic identity of free-living *Symbiodinium* obtained over a broad latitudinal range in the Japanese coast. *Phycol. Res.* **2013**, *61*, 68–80. [[CrossRef](#)]
25. Kang, N.S.; Jeong, H.J.; Moestrup, Ø.; Park, T.G. *Gyrodiniellum shiwhaense* n. gen., n. sp., a new planktonic heterotrophic dinoflagellate from the coastal waters of western Korea: Morphology and ribosomal DNA gene sequence. *J. Eukaryot. Microbiol.* **2011**, *58*, 284–309. [[CrossRef](#)] [[PubMed](#)]
26. Scholin, C.A.; Herzog, M.; Sogin, M.; Anderson, D.M. Identification of group and strain specific genetic makers for globally distributed *Alexandrium* (Dinophyceae) II. Sequence analysis of a fragment of the LSU rRNA gene. *J. Phycol.* **1994**, *30*, 999–1011. [[CrossRef](#)]
27. Litaker, R.W.; Vandersea, M.W.; Kibler, S.R.; Reece, K.S.; Stokes, N.A.; Steidinger, K.A.; Millie, D.F.; Bendis, B.J.; Pigg, R.J.; Tester, P.A. Identification of *Pfiesteria piscicida* (Dinophyceae) and *Pfiesteria*-like organisms using internal transcribed spacer-specific PCR assays. *J. Phycol.* **2003**, *39*, 754–761. [[CrossRef](#)]
28. Tamura, K.; Dudley, J.; Nei, M.; Kumar, S. MEGA4: Molecular evolutionary genetics analysis (MEGA) software v.4.0. *Mol. Biol. Evol.* **2007**, *24*, 1596–1599. [[CrossRef](#)]
29. Larkin, M.A.; Blackshields, G.; Brown, N.P.; Chenna, R.; McGettigan, P.A.; McWilliam, H.; Valentin, F.; Wallace, I.M.; Wilm, A.; Lopez, R.; et al. Clustal W and clustal X version 2.0. *Bioinformatics* **2007**, *23*, 2947–2948. [[CrossRef](#)]
30. Huelsenbeck, J.P.; Ronquist, F. MrBayes: Bayesian inference of phylogeny. *Bioinformatics* **2001**, *17*, 754–755. [[CrossRef](#)]
31. Ronquist, F.; Huelsenbeck, J.P. MRBAYES 3: Bayesian phylogenetic inference under mixed models. *Bioinformatics* **2003**, *19*, 1572–1574. [[CrossRef](#)]
32. Kang, N.S.; Jeong, H.J.; Moestrup, Ø.; Shin, W.G.; Nam, S.W.; Park, J.Y.; de Salas, M.F.; Kim, K.W.; Noh, J.H. Description of a new planktonic mixotrophic dinoflagellate *Paragymnodinium shiwhaense* n. gen., n. sp. from the coastal waters off western Korea: Morphology, pigments, and ribosomal DNA gene sequence. *J. Eukaryot. Microbiol.* **2010**, *57*, 121–144. [[CrossRef](#)]
33. Stamatakis, A. RAxML-VI-HPC: Maximum likelihood-based phylogenetic analyses with thousands of taxa and mixed models. *Bioinformatics* **2006**, *22*, 2688–2690. [[CrossRef](#)] [[PubMed](#)]
34. Breuer, G.; Evers, W.A.C.; de Vree, J.H.; Kleinegris, D.M.M.; Martens, D.E.; Wijffels, R.H.; Lamers, P.P. Analysis of fatty acid content and composition in microalgae. *J. Vis. Exp.* **2013**, *80*, e50628. [[CrossRef](#)] [[PubMed](#)]
35. Kang, N.S.; Lee, J.A.; Jang, H.S.; Kim, K.M.; Lim, E.S.; Yoon, M.; Hong, J.W. First record of a marine microalgal species, *Chlorella gloriosa* (Trebouxiophyceae) isolated from the Dokdo Islands, Korea. *Korean J. Environ. Biol.* **2019**, *37*, 526–534. [[CrossRef](#)]
36. Moestrup, Ø.; Lindberg, K.; Daugbjerg, N. Studies on woloszynskioid dinoflagellates IV: The genus *Biecheleria* gen. *Nov. Phycol. Res.* **2009**, *57*, 203–220. [[CrossRef](#)]
37. Fensome, R.A.; Taylor, F.J.R.; Norris, G.; Sargeant, W.A.S.; Wharton, D.I.; William, G.L. *A Classification of Living and Fossil Dinoflagellates*; Sheridan Press: Hanover, Germany, 1993; p. 351.
38. Gou, W.L.; Sun, J.; Li, X.Q.; Zhen, Y.; Xin, Z.; Yu, Z.G.; Li, R.X. Phylogenetic analysis of a free-living strain of *Symbiodinium* isolated from Jiaozhou Bay, P.R. China. *J. Exp. Mar. Biol. Ecol.* **2003**, *296*, 135–144. [[CrossRef](#)]
39. Jeong, H.J.; Yoo, Y.D.; Kang, N.S.; Lim, A.S.; Seong, K.A.; Lee, S.Y.; Lee, M.J.; Lee, K.H.; Kim, H.S.; Shin, W.G.; et al. Heterotrophic feeding as a newly identified survival strategy of the dinoflagellate *Symbiodinium*. *Proc. Natl. Acad. Sci. USA* **2012**, *109*, 12604–12609. [[CrossRef](#)]
40. Shao, P.; Chen, Y.Q.; Zhou, H.; Yuan, J.; Qu, L.H.; Zhao, D.; Lin, Y.S. Genetic variability in the Gymnodiniaceae ITS regions: Implications for species identification and phylogenetic analysis. *Mar. Biol.* **2004**, *144*, 215–224. [[CrossRef](#)]
41. McBride, B.B.; Muller-Parker, G.; Jakobsen, H.H. Low thermal limit of growth rate of *Symbiodinium californium* (Dinophyta) in culture may restrict the symbiont to southern populations of its host anemones (*Anthopleura* spp.; Anthozoa, Cnidaria). *J. Phycol.* **2009**, *45*, 855–863. [[CrossRef](#)]

42. Awai, K.; Matsuoka, R.; Shioi, Y. Lipid and fatty acid compositions of *Symbiodinium* strains. In Proceedings of the 12th International Coral Reef Symposium, Cairns, Australia, 9–13 July 2012.
43. Tsirigoti, A.; Tzovenis, I.; Koutsaviti, A.; Economou-Amilli, A.; Ioannou, E.; Melkonian, M. Biofilm cultivation of marine dinoflagellates under different temperatures and nitrogen regimes enhances DHA productivity. *J. Appl. Phycol.* **2020**. [[CrossRef](#)]
44. Mansour, M.P.; Volkman, J.K.; Jackson, A.E.; Blackburn, S.I. The fatty acid and sterol composition of five marine dinoflagellates. *J. Phycol.* **1999**, *35*, 710–720. [[CrossRef](#)]
45. Nichols, P.D.; Jones, G.J.; De Leeuw, J.W.; Johns, R.B. The fatty acid and sterol composition of two marine dinoflagellates. *Phytochemistry* **1984**, *23*, 1043–1047. [[CrossRef](#)]
46. Zhukova, N.V.; Aizdaicher, N.A. Fatty acid composition of 15 species of marine microalgae. *Phytochemistry* **1995**, *39*, 351–356. [[CrossRef](#)]
47. Volkman, J.K. Fatty acids of microalgae used as feedstocks in aquaculture. In *Fats for the Future*; Cambie, R.C., Ed.; Ellis Horwood: Chichester, UK, 1989; pp. 263–283.
48. Barreira, L.; Pereira, H.; Gangadhar, K.N.; Custódio, L.; Varela, J. Medicinal effects of microalgae-derived fatty acids. In *Handbook of Marine Microalgae*; Kim, S.K., Ed.; Academic Press: Cambridge, UK, 2015; pp. 209–231.
49. Mehta, L.R.; Dworkin, R.H.; Schwid, S.R. Polyunsaturated fatty acids and their potential therapeutic role in multiple sclerosis. *Nat. Clin. Pr. Neurol.* **2009**, *5*, 82–92. [[CrossRef](#)] [[PubMed](#)]
50. Helland, I.B.; Smith, L.; Saarem, K.; Saugstad, O.D.; Drevon, C.A. Maternal supplementation with very-long-chain n-3 fatty acids during pregnancy and lactation augments children’s IQ at 4 years of age. *Pediatrics* **2003**, *111*, e39–e44. [[CrossRef](#)] [[PubMed](#)]
51. Marszalek, J.R.; Lodish, H.F. Docosahexaenoic acid, fatty acid-interacting proteins, and neuronal function: Breastmilk and fish are good for you. *Annu. Rev. Cell Dev. Biol.* **2005**, *21*, 633–657. [[CrossRef](#)] [[PubMed](#)]
52. Jeromson, S.; Gallagher, I.J.; Galloway, S.D.; Hamilton, D.L. Omega-3 fatty acids and skeletal muscle health. *Mar. Drugs* **2015**, *13*, 6977–7004. [[CrossRef](#)] [[PubMed](#)]
53. Kang, J.X. Omega-3: A link between global climate change and human health. *Biotechnol. Adv.* **2011**, *29*, 388–390. [[CrossRef](#)]
54. Jang, H.S.; Kang, N.S.; Kim, K.M.; Jeon, B.H.; Park, J.S.; Hong, J.W. Description and application of a marine microalga *Auxenochlorella protothecoides* isolated from Ulleung-do. *J. Life Sci.* **2017**, *27*, 1152–1160.
55. Kim, K.M.; Kang, N.S.; Jang, H.S.; Park, J.S.; Jeon, B.H.; Hong, J.W. Characterization of *Heterochlorella luteoviridis* (Trebouxiaceae, Trebouxiophyceae) isolated from the Port of Jeongja in Ulsan, Korea. *J. Mar. Biosci. Biotechnol.* **2017**, *9*, 22–29.
56. Manikan, V.; Nazir, M.Y.M.; Kalil, M.S.; Isa, M.H.M.; Kader, A.J.A.; Yusoff, W.M.W.; Hamid, A.A. A new strain of docosahexaenoic acid producing microalga from Malaysian coastal waters. *Algal Res.* **2015**, *9*, 40–47. [[CrossRef](#)]
57. Thompson, P.A.; Guo, M.X.; Harrison, P.J.; Whyte, J.N. Effects of variation in temperature. II. On the fatty acid composition of eight species of marine phytoplankton. *J. Phycol.* **1992**, *28*, 488–497. [[CrossRef](#)]
58. Patterson, E.; Wall, R.; Fitzgerald, G.F.; Ross, R.P.; Stanton, C. Health implications of high dietary ω -6 polyunsaturated Fatty acids. *J. Nutr. Metab.* **2012**, *2012*, 539426. [[CrossRef](#)] [[PubMed](#)]
59. Simopoulos, A.P. The importance of the ω -6/ ω -3 fatty acid ratio in cardiovascular disease and other chronic diseases. *Exp. Biol. Med. (Maywood)* **2008**, *233*, 674–688. [[CrossRef](#)] [[PubMed](#)]
60. FAO. *The State of World Fisheries and Aquaculture 2018—Meeting the Sustainable Development Goals*; FAO: Rome, Italy, 2018.
61. Turchini, G.M.; Ng, W.K.; Tocher, D.R. *Fish oil replacement and alternative lipid sources in aquaculture feeds*; Taylor & Francis, CRC Press: Boca Raton, FL, USA, 2010; p. 533.
62. De Roos, B.; Sneddon, A.A.; Sprague, M.; Horgan, G.W.; Brouwer, I.A. The potential impact of compositional changes in farmed fish on its health-giving properties: Is it time to reconsider current dietary recommendations? *Public Health Nutr.* **2017**, *20*, 2042–2049. [[CrossRef](#)]
63. Sprague, M.; Dick, J.R.; Tocher, D.R. Impact of sustainable feeds on omega-3 long-chain fatty acid levels in farmed Atlantic salmon, 2006–2015. *Sci. Rep.* **2016**, *6*, 21892. [[CrossRef](#)]
64. Chen, M.; Liu, H.; Chen, B. Effects of dietary essential fatty acids on reproduction rates of subtropical calanoid copepod, *Acartia erythraea*. *Mar. Ecol. Prog. Ser.* **2012**, *455*, 95–110. [[CrossRef](#)]

65. Jonasdottir, S.H. Effects of food quality on the reproductive success of *Acartia tonsa* and *Acartia hudsonica*—Laboratory observations. *Mar. Biol.* **1994**, *121*, 67–81. [[CrossRef](#)]
66. Taipale, S.J.; Kahilainen, K.K.; Holtgrieve, G.W.; Peltomaa, E.T. Simulated eutrophication and browning alters zooplankton nutritional quality and determines juvenile fish growth and survival. *Ecol. Evol.* **2018**, *8*, 2671–2687. [[CrossRef](#)]



© 2020 by the authors. Licensee MDPI, Basel, Switzerland. This article is an open access article distributed under the terms and conditions of the Creative Commons Attribution (CC BY) license (<http://creativecommons.org/licenses/by/4.0/>).